Invadolysin: a novel, conserved metalloprotease links mitotic structural rearrangements with cell migration

Published November 22, 2004

Invadolysin: a novel, conserved metalloprotease links mitotic structural rearrangements with cell migration

Brian McHugh,[1] Sue A. Krause,[1] Bin Yu,[1] Anne-Marie Deans,[1] Sarah Heasman,[2] Paul McLaughlin,[1] and Margarete M.S. Heck[1]

[1]Wellcome Trust Centre for Cell Biology, University of Edinburgh, Edinburgh EH9 3JR, Scotland, UK
[2]Medical Research Council Centre for Inflammation Research, University of Edinburgh, Edinburgh EH8 9AG, Scotland, UK

The cell cycle is widely known to be regulated by networks of phosphorylation and ubiquitin-directed proteolysis. Here, we describe IX-14/invadolysin, a novel metalloprotease present only in metazoa, whose activity appears to be essential for mitotic progression. Mitotic neuroblasts of *Drosophila melanogaster IX-14* mutant larvae exhibit increased levels of nuclear envelope proteins, monopolar and asymmetric spindles, and chromosomes that appear hypercondensed in length with a surrounding halo of loosely condensed chromatin. Zymography reveals that a protease activity, present in wild-type larval brains, is missing from homozygous tissue, and we show that IX-14/invadolysin cleaves lamin in vitro. The IX-14/invadolysin protein is predominantly found in cytoplasmic structures resembling invadopodia in fly and human cells, but is dramatically relocalized to the leading edge of migrating cells. Strikingly, we find that the directed migration of germ cells is affected in *Drosophila IX-14* mutant embryos. Thus, invadolysin identifies a new family of conserved metalloproteases whose activity appears to be essential for the coordination of mitotic progression, but which also plays an unexpected role in cell migration.

Introduction

Recent years have witnessed remarkable strides in our understanding of the control of cell cycle progression. It is now clear that cell cycle progression is driven by the successive activation and inactivation of the Cdks, and that abrupt transitions are often enforced by the cleavage of key targets by the proteasome after their ubiquitination by various E3 ubiquitin ligases (for review see Murray, 2004). Cdk phosphorylation of key components regulates the entry of cells into S phase and choreographs the subsequent firing of replication origins. Entry into mitosis is also determined by Cdks, and Cdk phosphorylation of the nuclear lamins drives the cycle of nuclear envelope disassembly and reassembly that is characteristic of mitosis in metazoa. The exit from mitosis is triggered not only by proteolysis of mitotic cyclins but also of securin leading to the activation of separase, a CD clan protease that cleaves the rad21/Scc1 non-structural maintenance of chromosomes cohesin subunit, thereby triggering the separation of sister chromatids.

One aspect of mitosis about which we still know relatively little is the process of mitotic chromosome formation. The compaction of chromatin into mitotic chromosomes is essential to avoid sister chromatid entanglement and cleavage of chromatin at cytokinesis. Recent breakthroughs, such as the discovery of the structural maintenance of chromosomes–containing condensin complex, at first appeared to provide the key, but recent analyses of condensin mutations and RNAi depletions have revealed that mitotic chromosomes form even in the absence of condensin subunits (Bhat et al., 1996; Steffensen et al., 2001; Coelho et al., 2003; Hudson et al., 2003). Further evidence suggests that correct mitotic chromosome condensation is linked to replication timing and checkpoint control (Loupart et al., 2000; Krause et al., 2001; Pflumm and Botchan, 2001). Thus, the search for factors that give the mitotic chromosome its characteristic form and integrity is still very much on.

The online version of this article includes supplemental material.

Correspondence to M.M.S. Heck: margarete.heck@ed.ac.uk

B. McHugh's present address is Medical Research Council Centre for Inflammation Research, University of Edinburgh, Edinburgh EH8 9XD, UK.

S.A. Krause's present address is University of Glasgow, Institute of Biological and Life Sciences, Glasgow G11 6NU, UK.

A.-M. Deans's present address is Institute of Immunology and Infection Research, University of Edinburgh, Edinburgh EH9 3JT, UK.

Abbreviations used in this paper: MMP, matrix metalloproteases; S2, Schneider 2.

Supplemental Material can be found at:
http://jcb.rupress.org/content/suppl/2004/11/22/jcb.200405155.DC1.html

The Journal of Cell Biology, Vol. 167, No. 4, November 22, 2004 673–686
http://www.jcb.org/cgi/doi/10.1083/jcb.200405155

Published November 22, 2004

This work began as part or our ongoing characterization of *Drosophila melanogaster* mutations that are defective in mitotic chromosome condensation. Mitotic events are particularly amenable to study in *Drosophila* as many mutations affecting mitosis are lethal only at the late larval stages due to the maternal store of proteins in the embryo and the fact that larvae do not require mitotic activity for growth and development. This allows the use of mitotically active tissues such as larval brains and imaginal discs for studying proliferation in wild-type and mutant states (Gatti and Baker, 1989; Theurkauf and Heck, 1999). As a result, *Drosophila* has proven useful both for the characterization of known cell cycle regulators (O'Farrell et al., 1989; Edgar and Lehner, 1996; Fogarty et al., 1997; Sibon et al., 1997; Jager et al., 2001) and for the identification of novel factors, such as the polo and aurora kinases that have subsequently proven to be important for cell cycle regulation in diverse organisms (Sunkel and Glover, 1988; Llamazares et al., 1991; Glover et al., 1995).

We examined the *l(3)IX-14* mutation because of its dramatic effects on mitotic chromosome formation, distinct from other mitotic mutations. Our detailed analyses have revealed the gene to be important for other aspects of mitosis, including spindle assembly and nuclear envelope dynamics. Furthermore, the identification of the gene and characterization of its higher eukaryotic counterparts led to several surprises. The *IX-14* gene encodes a metalloprotease that is concentrated in cytoplasmic structures resembling invadopodia. Invasive tumor cells have the ability to elaborate invadopodia that facilitate extracellular matrix degradation, thus aiding metastasis (Bowden et al., 2001; Buccione et al., 2004). The IX-14 protein is structurally related to leishmanolysin, a major surface protease from *Leishmania* protozoa, which is thought to have a significant role in the pathogenesis of leishmaniasis (Yao et al., 2003). As a result of the subcellular localization and the sequence homology, we have termed the protein product of the IX-14 gene "invadolysin." We have discovered that invadolysin is highly concentrated at the leading edge of migrating macrophages. Consistent with a role in cell migration, we observe that the active migration of primordial germ cells is affected in mutant fly embryos. Thus, IX-14/invadolysin, a member of a new class of metalloproteases, links mitosis with cell migration.

Results

Chromosome structure is disrupted in the *IX-14* mutation

l(3)IX-14^{1} is a late larval lethal mutation on the right arm of the third chromosome, generated in an ICR-170 chemical mutagenesis screen for imaginal disc mutations (Shearn et al., 1971). Preliminary analysis reported that the mutation was characterized by metaphase arrest and hypercondensed mitotic chromosomes (Gatti and Baker, 1989). We generated a transposon insertion allele of the gene, *l(3)IX-14*^{4Y7}, by local hopping of a nearby P-element insertion. Here, we report a detailed phenotypic analysis of both alleles, investigating not only chromosome morphology but also other aspects of cell division.

Whole mount preparations of *IX-14* third instar larval brains and imaginal discs showed that mutant tissues had proliferation defects resulting in much-reduced brain size and missing imaginal discs (unpublished data). Fig. 1 shows typical DAPI-stained mitotic figures observed in wild-type (Fig. 1 A) and in *IX-14* mutant (Fig. 1 C) neuroblasts. The *IX-14* neuroblasts show the length-wise hypercondensation of mitotic chromosomes initially observed after orcein staining, but additionally demonstrate that the mutant chromosomes appear loosely condensed with a ragged periphery. This phenotype differs from the extreme hypercondensation in other mutations that produce a mitotic arrest phenotype (Heck et al., 1993) or treatment of wild-type cells with microtubule poisons such as colchicine (Fig. 1 B). Allowing more time in mitosis with colchicine does not rescue the lateral condensation defect in *IX-14* mutant neuroblasts (Fig. 1 D), thus we believe the phenotype represents a specific condensation defect rather than "conventional" hypercondensation in response to mitotic delay.

The *IX-14* mutation affects interphase polytene chromosomes as well as mitotic chromosomes. Polytene chromosomes from salivary glands of wild-type third instar larvae are distinctively banded along the chromosome arms, and the centromeres of the endo-reduplicated chromosomes are clustered at the chromocenter (Fig. 1 E). This characteristic banding pattern is abolished in *IX-14* mutant polytenes and the chromosome arms appear twisted and frayed (Fig. 1 F). In many nuclei it is difficult to identify an obvious chromocenter. Additionally, mutant polytenes were approximately half the size seen in wild type. This reduction in size may be due to under-replication, as BrdU incorporation is clearly reduced in *IX-14* mutant neuroblasts, though the structural defects are not merely explicable by reduced replication.

To further investigate an effect of the *IX-14* mutation on interphase chromatin structure suggested by the polytene phenotype, we addressed whether or not this mutation might act as a modifier in a position effect variegation assay. We examined the effect of one copy of each *IX-14* allele on expression of the *white* gene in a *white mottled 4* (w^{m4}) background. In w^{m4}, inversion of much of the X chromosome places the *white* gene (expression of which is responsible for normal red eye color) adjacent to heterochromatin, thereby reducing its expression. Mutations that enhance variegation, E(var)s, further reduce expression of the *white* gene (whiter eyes) potentially by increasing the "spreading" of heterochromatin. Suppressors of variegation, Su(var)s, result in greater expression of the *white* gene (redder eyes) by decreasing the heterochromatic environment of the reporter gene. Fig. 1 G shows a pronounced increase in the redness of flies' eyes with one copy of each *IX-14* allele in a w^{m4} background, indicating that *IX-14* alleles are acting as Su(var)s and "opening" heterochromatin. By inference, one role of wild-type IX-14 may be to promote chromatin compaction or heterochromatin formation, which is consistent with the observed mitotic defects. Therefore, we conclude that IX-14 is required for chromosome architecture during both mitosis and interphase.

Published November 22, 2004

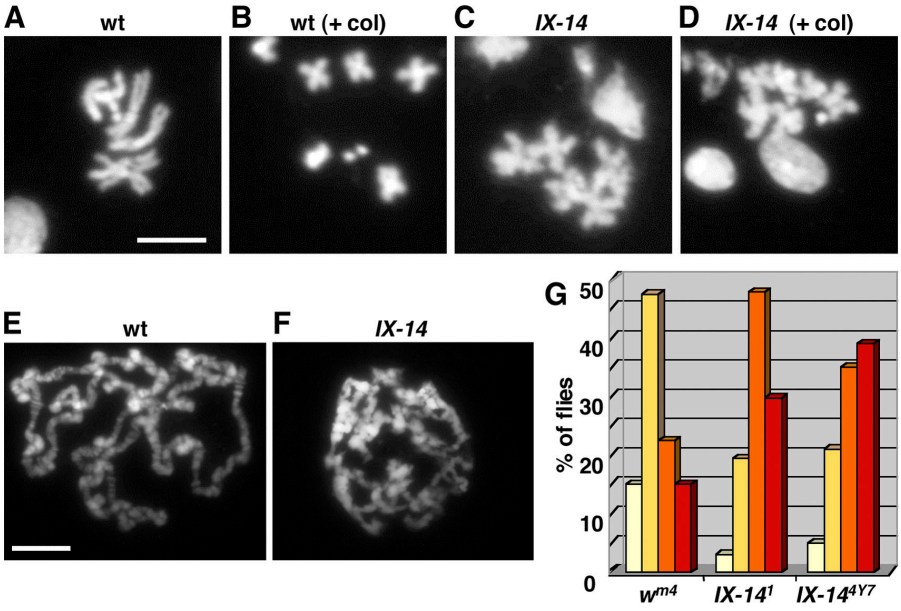

Figure 1. **Chromosome defects in *l(3)IX-14*.** (A–D) Mitotic chromosome spreads from wild-type (wt) and homozygous *l(3)IX-14* mutant (*IX-14*) third instar larval brains. "+ col" denotes images from the representative genotype after treatment with colchicine for 90 min. Note that even with colchicine treatment, the *IX-14* chromosomes are unable to condense as tightly as the wild-type chromosomes. Bar, 5 μm. (E and F) Polytene chromosome spreads from wild-type and *IX-14* homozygous mutant third instar larval salivary glands. Banding and a chromocenter are not as obvious in the mutant chromosomes. Bar, 10 μm. (G) Position effect variegation assay using "white" as a reporter gene (w^{m4}). Flies were sorted into categories based on redness of the adult eyes (white bars, 0–25% redness; yellow bars, 26–50% redness; orange bars, 51–75% redness; red bars, 76–100% redness). The distribution of eye color is shown for the original w^{m4} stock as well as for w^{m4} stocks containing one copy of each of the two mutant *l(3)IX-14* alleles. The majority of w^{m4};*l(3)IX-14* (both alleles) flies grouped toward the red end of the spectrum, implying that the mutant alleles act as suppressors of variegation (enhancing expression of the reporter gene) and, conversely, that the wild-type gene product acts to compact chromatin.

Spindle and centrosomal abnormalities are common in *IX-14* mutants

The over-shortened mitotic chromosomes suggested that *IX-14* mutants may experience a metaphase delay possibly caused by aberrant spindles. Neuroblasts of *IX-14* mutants indeed exhibited abnormal spindle morphology (Fig. 2, B–D and F), and in fact only 2% of mitotic cells had a normal bipolar spindle. Spindle abnormalities included monopolar spindles (37%; Fig. 2 B, inset 1), disorganized spindles (34%; Fig. 2 B, insets 2 and 3), and mitotic figures where the spindle appeared bipolar, but asymmetric (27%, Fig. 2 C, inset 4). Mutant spindles also appeared to have thicker bundles of microtubules, compared with the finer fibers observed in wild type (Fig. 2 A). Almost no anaphase figures were observed in DAPI-stained neuroblasts from *IX-14* mutant larvae, which is consistent with a metaphase delay or arrest.

Nearly 70% of mitotic figures in *IX-14* neuroblasts appeared to have only one focus of centrosomal staining, as judged by CP190 localization (Fig. 2, B–D and F). Cells with monopolar spindles always had a single centrosome, whereas 75% of the asymmetric bipolar spindles also had only one CP190 "spot" (Fig. 2 G). This single centrosome phenotype was also verified with another mitotic centrosomal marker, centrosomin (unpublished data). In many cases, centrosomes appeared to have a dumbbell shape (Fig. 2 F, arrow), suggesting that centrosomes had duplicated but not separated. Although CP190 normally has a nuclear localization during interphase (binding to specific loci on polytenes), the protein dissociates from chromosomes in mitosis (Whitfield et al., 1995). Mitotic chromosomes from *IX-14* homozygous cells curiously appeared to have higher levels of CP190 than wild-type chromosomes (Fig. 2 F).

The aberrant spindles in the *IX-14* mutation afford an explanation for the length-wise hypercondensation of chromosomes, as spindle defects would be expected to arrest cells in mitosis. However, the loose compaction and ragged edges of the chromosomes cannot be accounted for by spindle abnormalities as this is not observed when cells are arrested in mitosis in response to microtubule poisons or other spindle defects (Heck et al., 1993). Thus, IX-14 has essential roles both in chromosome and spindle architecture in *Drosophila* cells.

IX-14 mutant mitotic cells accumulate abnormally high levels of nuclear envelope proteins

As higher eukaryotic cells enter mitosis, chromosome condensation and spindle assembly are accompanied by the disassembly of the nuclear envelope. Surprisingly, the majority of *IX-14* mitotic cells showed dramatically increased levels of lamin Dm0 (a B-type lamin), compared with wild-type mitotic cells (Fig. 3, A and B). Strikingly, the level of another *Drosophila* nuclear envelope protein, otefin, also appeared elevated in *IX-14* mitotic cells (Fig. 3, C and D). When double immunofluorescence was performed, we observed a simultaneous increase of lamin and otefin in the same cells (unpublished data). We believe this elevation occurs before mitosis as late G2 cells (those positive for mitosis-specific phosphorylation of Serine 10 on histone H3) also exhibited increased lamin and otefin fluorescence.

The increase in immunofluorescence corresponds to an actual increase in protein level. Immunoblotting for lamin Dm0 and otefin very clearly showed that these proteins accumulated to unusually high levels in *IX-14* larval brains (compare with the α-tubulin loading control in Fig. 3 [E and F]). We additionally detected an increase in the level of *Drosophila* lamin C (unpublished data). We only detected increase of full-length forms by immunoblotting, with no evidence for accumulation of alternative forms. Merely arresting wild-type cells in mitosis with colchicine did not elevate lamin levels (unpublished data).

Published November 22, 2004

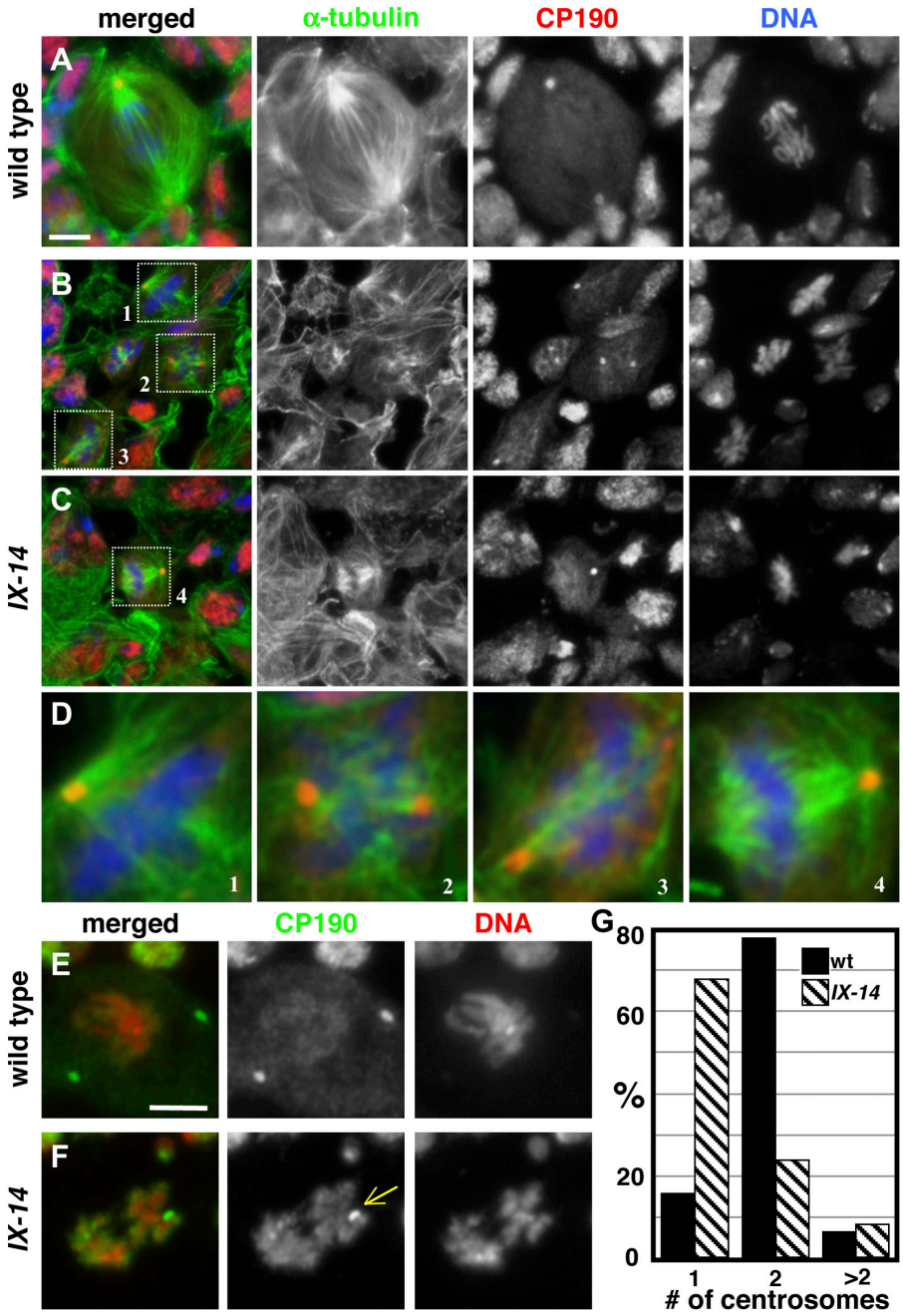

Figure 2. **Centrosome and spindle phenotypes of *l(3)IX-14*.** (A) Wild-type larval neuroblasts stained for α-tubulin (green), CP190 (red), and DAPI (blue). Wild-type metaphase figures contain normal bipolar spindles with two centrosomes. (B–D) *IX-14* larval neuroblasts labeled as in A show extreme spindle abnormalities. Boxed mitotic figures in *IX-14* mutant panels are enlarged in D to highlight mutant phenotypes of monopolar (1), disorganized (2 and 3), and asymmetric (4) spindles. Bar, 5 μm. (E) Wild-type larval neuroblasts stained for CP190 (green) and DAPI (red), showing duplicated and separated centrosomes at metaphase. (F) *IX-14* larval neuroblast stained as in E, showing chromosome condensation and centrosome separation defects (arrow) in mitosis. Additionally, CP190 appears to persist on *IX-14* mutant chromosomes longer than in wild-type cells. Bar, 5 μm. (G) Quantitation of centrosome number in the wild-type and *IX-14* mitotic cells. Nearly 70% of mitotic figures in the *IX-14* mutation appeared to have only one focus of centrosomal staining.

We conclude that the *IX-14* mutation appears to affect multiple aspects of structural rearrangement as cells enter mitosis.

The *IX-14* gene encodes a novel metalloprotease

We mapped the original *IX-14* allele to the 85E10-F16 region by crossing to deficiency lines with known breakpoints. We then generated a P-element insertion allele by local hopping a nearby P-element, *l(3)04017*. The P-element allele allowed cloning of adjacent genomic DNA by inverse PCR; hybridization of this fragment to a *Drosophila* P1 array refined our mapping to 85F14-15. A candidate *IX-14* gene was cloned by identifying a 3.6-kb full-length *Drosophila* adult head library EST whose sequence overlapped with the ~700-bp genomic fragment flanking the P-element. The gene was composed of nine exons, with the first exon separated from the remaining eight by a large (~8.6 kb) intron (Fig. 4 A, asterisk). This gene has been designated CG3953 in the *Drosophila* genome annotation database.

We mapped the P-element insertion site to 40 bp upstream of the start of transcription of the *IX-14* gene. Precise excision of this P-element was shown to revert the mutant phenotype and restore viability. The insertion appeared to disrupt the *IX-14* promoter, resulting in a strong hypomorphic or null mutation. To determine whether or not expression of this gene was affected in *IX-14* alleles, Northern blot analysis was performed on total RNA from third instar larvae. This showed that the predicted 3.6-kb mRNA was indeed missing in larval extracts prepared from both *IX-14* alleles (Fig. 4 B).

Published November 22, 2004

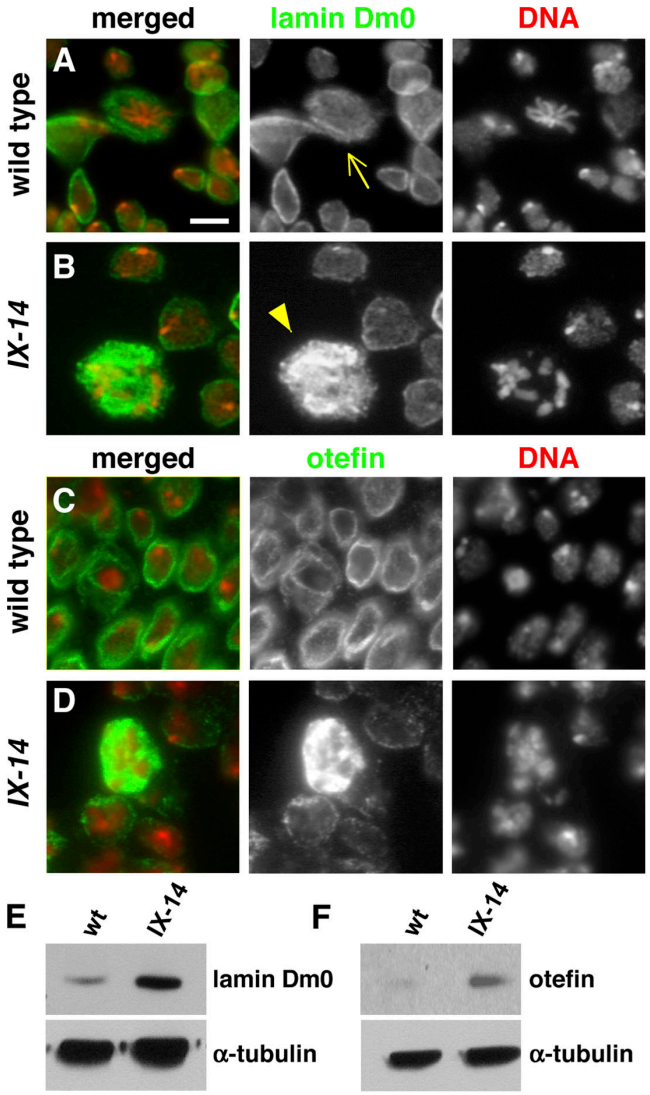

Figure 3. **Abnormal levels of nuclear envelope proteins in *l(3)IX-14* mutant cells.** Larval brains from wild-type and *IX-14* homozygous mutant animals were processed for lamin and otefin detection. (A) Wild-type mitotic cells (arrow) show homogeneous lamin staining as the nuclear lamina becomes dispersed during mitosis. (B) In contrast, both *IX-14* alleles have greatly increased lamin staining during mitosis (arrowhead). Bar, 5 μm. (C) Wild-type neuroblasts show distinct nuclear envelope staining similar to lamin. (D) Both *IX-14* alleles also show greatly increased otefin staining during mitosis. Protein extracts from wild-type and *IX-14* larval brains were probed for Dm0 lamin (E) and otefin (F). α-tubulin (bottom) served as a loading control, and confirmed that the samples were similarly loaded. The levels of both lamin and otefin detectable by immunoblotting was significantly greater in the mutant tissues than in wild-type brains.

The 2,052 nucleotide ORF in the *IX-14* cDNA encodes a 683 amino acid protein (predicted M_r = 71 kD) with homology to proteins in the M8 class of zinc-metalloproteases focused on the characteristic "HEXXHXXG[X]$_N$H" catalytic motif. The founding member of this family is the leishmanolysin cell surface protein (also called GP63) from the pathogen *Leishmania major*. In vitro mutagenesis of leishmanolysin has determined that the glutamic acid and three histidine residues are essential for protease activity (McMaster et al., 1994; Macdonald et al., 1995; McGwire and Chang, 1996). We have been able to identify orthologues in all higher eukaryotes examined, but conspicuously not in bacteria or yeasts, suggesting that the IX-14 gene product may only be required in metazoa.

The worm, human, mouse, and fly orthologues are shown in the alignment of Fig. 4 C, but other more divergent orthologues (e.g., *Arabidopsis thaliana* and *Dictyostelium discoideum*) are not included. Although the most obvious homology with leishmanolysin is centered on the conserved zinc-metalloprotease motif (Fig. 4 C, boxes) and immediate surrounding regions, the NH_2- and COOH-terminal regions are considerably more divergent. A potential signal sequence is present near the NH_2 terminus of all orthologues, although whether or not this sequence acts to target the protein is currently unknown. Intriguingly, there are at least nine blocks (Fig. 4 C, numbered double-headed arrows) shared among the worm, human, mouse, and fly orthologues that are absent from the leishmanolysin sequence. Despite this finding, the positions of 14 cysteines are remarkably conserved between leishmanolysin and the higher eukaryotic proteins (Fig. 4 C, asterisks). This result suggests strongly that the "core" of the IX-14 protease should resemble that of leishmanolysin (Schlagenhauf et al., 1998), and furthermore predicts that the indicated "insertions" should lie at the surface of this structure. Indeed, the sites of these insertions all map to the surface of the leishmanolysin structure (Fig. 4 D, black numbered spheres; the internal zinc ion essential for catalysis is represented by a magenta sphere). Therefore, we conclude that IX-14 is a member of a subgroup of the leishmanolysin protease group.

RNAi depletion of IX-14 in cultured cells phenocopies neuroblast defects

As further evidence that the gene we identified is responsible for the defects observed in *IX-14* larval tissues, we performed dsRNA-mediated interference of *IX-14* in *Drosophila* Schneider 2 (S2) cells. The abnormal spindle phenotypes seen in the mutant alleles, typically monopolar or disorganized, were phenocopied in roughly 25% of the *IX-14* RNAi mitotic cells (Fig. 5 A). In addition, mitotic figures from RNAi cultures were frequently observed to have single centrosomes or what appeared to be two closely apposed centrosomes (Fig. 5 B). Although control S2 cells have a low level of aneuploidy and occasional abnormal numbers of centrosomes, neither the aberrant spindles nor unseparated centrosomes were observed in control cells (Fig. 5, −dsRNA panels). Therefore, we are confident that loss of the IX-14 protein is responsible for the observed cellular phenotypes.

IX-14 cleaves lamin in vitro

To examine whether or not IX-14 has protease activity, suggested by its homology to the catalytic motif of leishmanolysin, we performed two complementary approaches. In the first, protein extracts prepared from wild-type and *IX-14* mutant larval brains were examined for protease activity (Fig. 6 A). Protease activity was assayed in zymogram gels containing casein as substrate. Whole larvae harbor a high level of protease activity at numerous molecular masses when assessed by zymography (unpublished data). Therefore, we prepared protein extracts

Published November 22, 2004

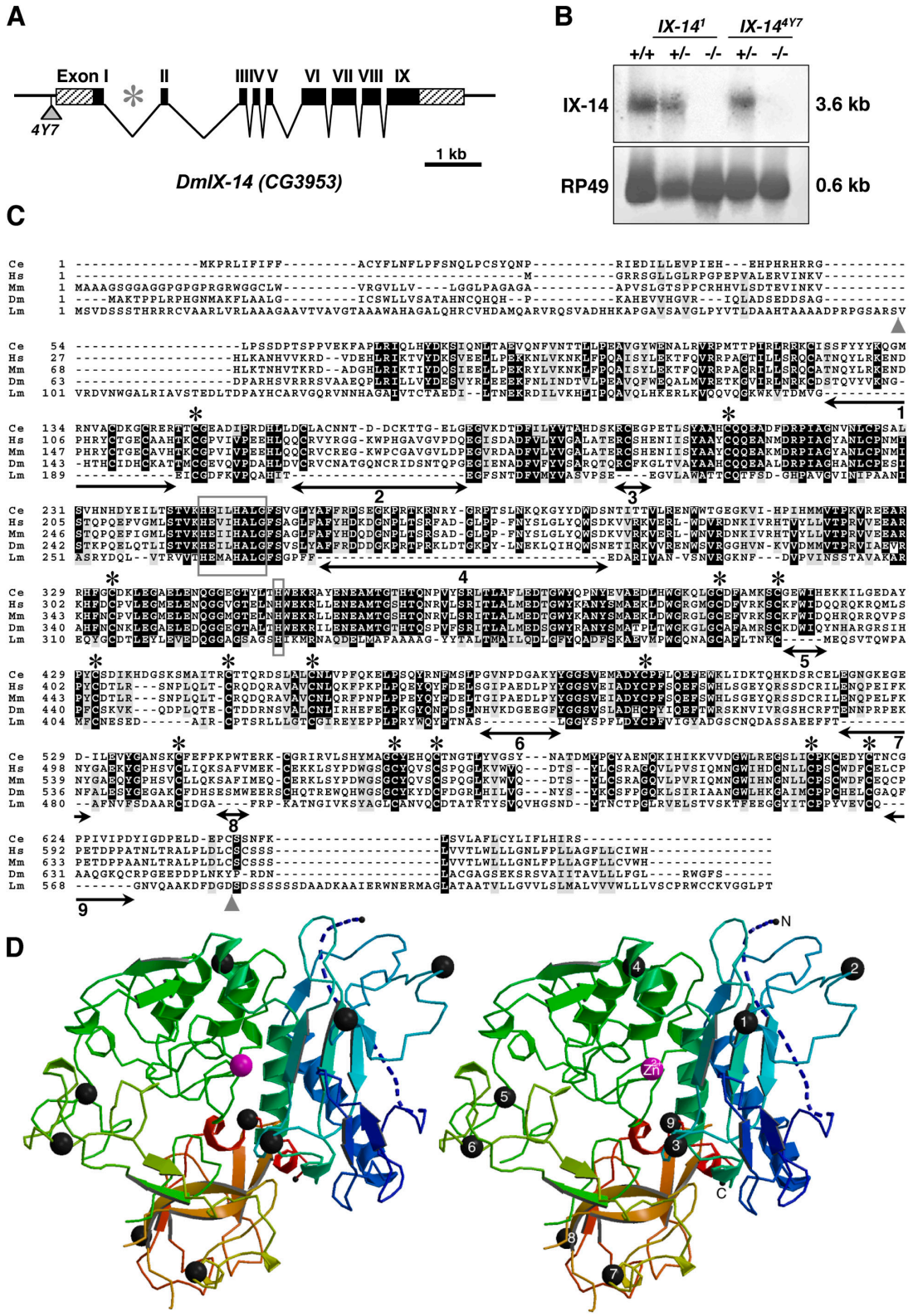

Figure 4. **Molecular characterization of *l(3)IX-14.*** (A) Map of the DmIX-14 gene (CG3953), with exons depicted as black boxes and 5′ and 3′ UTRs as hatched boxes. The position of the P element insertion in *l(3)IX-14*^{4Y7} is 40 bp upstream of the transcription start site (gray triangle). The first intron (8.6 kb, asterisk) is not shown to scale in this figure. (B) Northern blot of wild type and *IX-14* heterozygous (+/−) and homozygous (−/−) total larval RNA probed with IX-14 full-length cDNA. The same blot probed for ribosomal protein RP49 mRNA is shown as a control. The IX-14 mRNA is undetectable in RNA obtained from homozygous *IX-14* alleles. (C) T-COFFEE alignment showing homology between *Drosophila melanogaster* IX-14, metazoan orthologues, and Leishmanolysin, with the conserved HEXXHXXG (and third required H) zinc-metalloprotease motif boxed. Sequences shown are as follows: Ce, *Caenorhabditis elegans* (CAB16471); Hs, *Homo sapiens* (CAC42882); Mm, *Mus musculus* (NP 766411); Dm, *Drosophila melanogaster* (NP 652072); Lm, *Leishmania major* (AF039721). Although the homology between leishmanolysin and the other proteins appears to be largely limited to regions surrounding the metalloprotease motif, the placement of 14 cysteines (asterisks) is strikingly conserved. Nine regions shared among the higher eukaryotic ortho-

Published November 22, 2004

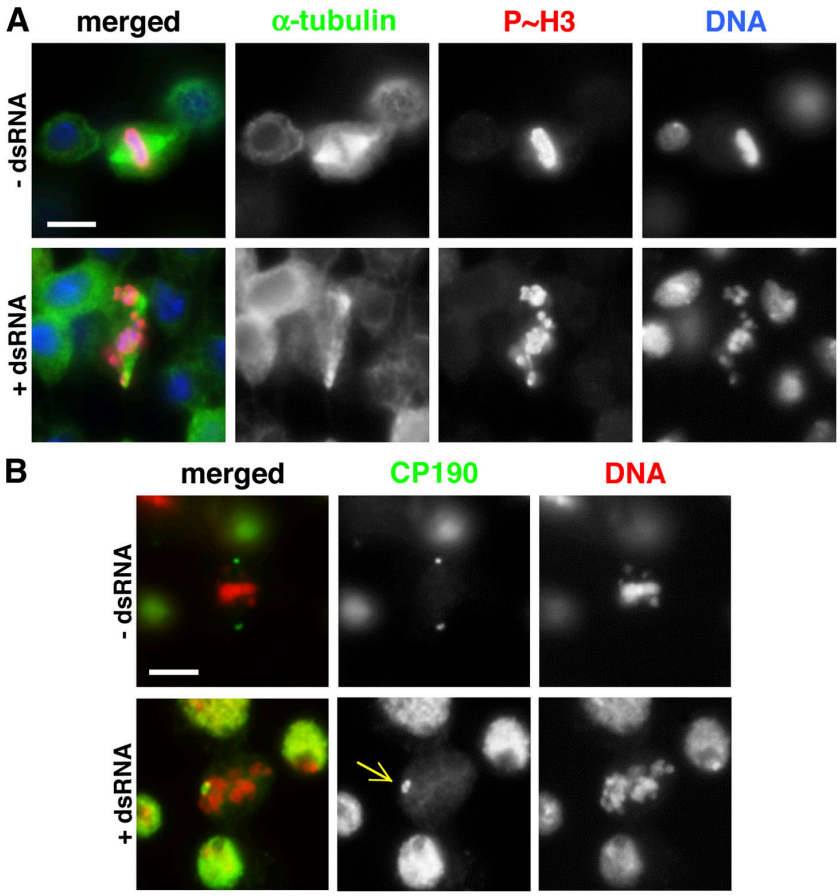

Figure 5. **dsRNA-mediated interference of IX-14 in *Drosophila* S2 cells phenocopies the mutation.** (A) Spindles of S2 cells: control (top) and 72 h after dsRNA treatment (bottom). Cells are stained for α-tubulin (green), P~H3 (red), and DAPI (blue). The normal bipolar spindle in the control S2 cell is to be contrasted with the disorganized spindle shown in the treated cell. This is similar to that observed in *IX-14* homozygous mutant alleles. Bar, 5 μm. (B) Centrosomes of S2 cells: control (top) and 72 h after dsRNA treatment (bottom). Cells are stained for CP190 (green) and DAPI (red). The treated cells show the centrosome separation defect (arrow) similar to that observed in *l(3)IX-14* homozygous mutant alleles. Bar, 5 μm.

from larval brains only, as the phenotypes were clearly apparent in this proliferating tissue. Wild-type brain lysates had two visible bands of protease activity, migrating at ~120 and 135 kD (Fig. 6 A, asterisks). Remarkably, these two bands of activity were almost completely absent in *IX-14* brains, indicating that mutant extracts were indeed missing proteolytic activity. A separate stained gel documents that wild-type and mutant lanes were equivalently loaded (Fig. 6 B). As these zymogram gels are nondenaturing, the molecular mass of the observed activity is not necessarily related to predicted molecular mass, but may suggest that IX-14 migrates as a multimer or part of a complex. The lack of protease activity in mutant brains further suggests that the IX-14 gene product is responsible not only for the mutant phenotypes but also for the protease activity observed under these conditions (either directly or potentially through the activation of other proteases).

The increase in nuclear envelope proteins observed by immunofluorescence and immunoblotting in mutant brains suggested that lamin (or otefin) might be a substrate of the IX-14 metalloprotease. As shown in Fig. 6 C, in vitro synthesized Dm0 lamin is cleaved by in vitro synthesized IX-14. Furthermore, the cleavage of lamin can be inhibited by the inclusion of ortho-phenanthroline, a chelator of zinc (Fig. 6 C, asterisks). Although full-length lamin was detected by immunoblotting in this experiment (Fig. 6 C, arrowhead), we failed to detect any cleavage products (they may not be recognized by the antibody used). Thus, IX-14 is a novel essential protease capable of cleaving at least one component of the nuclear envelope.

IX-14 localizes to distinct structures in the cytoplasm of *Drosophila* and human cells

Several approaches were used to determine the subcellular localization of the IX-14 protein. *Drosophila* S2 cells transiently transfected with expression plasmids tagging either the NH_2 or COOH terminus with EGFP showed cytoplasmic localization, whereas vector alone localized to both the nucleus and cytoplasm (Fig. 7 A). The human genome contains a single *IX-14* gene, which we have shown by preliminary siRNA analysis to be essential for viability (unpublished data). Due to the limit of resolution with the relatively small and generally nonadherent S2 cells, we turned to examining IX-14 localization in human cells. A COOH-terminal EGFP fusion construct of HsIX-14 in HeLa cells was also localized

logues (absent from leishmanolysin) are indicated by double-headed arrows. The gray triangles delimit the region of the leishmanolysin protein that is shown in D. (D) Stereo pair of the three-dimensional structure of leishmanolysin is shown (PDB accession code is 1LML). The black numbered spheres represent the higher eukaryotic "insertions" (relative to leishmanolysin), which all map to the surface of the leishmanolysin structure. The internal magenta sphere represents the zinc ion required for catalysis.

Published November 22, 2004

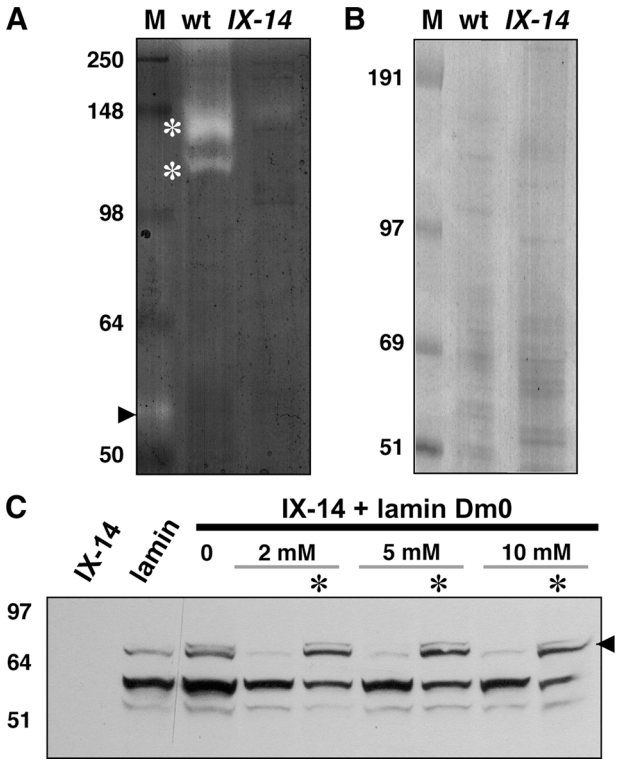

Figure 6. **The IX-14 protein exhibits protease activity.** (A) Colloidal Coomassie blue–stained nondenaturing casein zymogram gel showing one brain equivalent of wild type (+/+) versus three brain equivalents of homozygous (*IX-14*) third instar larval brain extract. A doublet of protease activity is observed in wild-type extracts (asterisks), but is greatly depleted in mutant extracts. A band of protease activity is also present in the prestained molecular mass markers (arrowhead), which serves as an internal control in these experiments. (B) Coomassie blue–stained denaturing polyacrylamide gel showing equivalent loading of larval brain extracts (three mutant brains are a roughly equivalent amount to one wild-type brain). (C) *Drosophila* IX-14 cleaves *Drosophila* Dm0 lamin in vitro. In vitro transcribed and translated proteins were mixed and incubated for 60 min at 29°C (IX-14 and lamin alone are in the first two lanes). The cleavage of lamin was detected by immunoblotting with a mAb generated against the NH_2-terminal head region (arrowhead). The addition of zinc at 2, 5, or 10 mM enhanced the cleavage reaction, whereas the addition of the 1,10-phenanthroline zinc chelator inhibited the cleavage of lamin by the IX-14 protease (asterisks).

in the cytoplasm, often as unusual ring-like structures (Fig. 7 B). A control transfection with EGFP alone localized throughout both the nucleus and cytoplasm. From these experiments we concluded that the IX-14 protein localized predominantly in the cytoplasm of fly and human cells.

Two protein sequences for the human orthologue possibly representing alternatively spliced forms have been submitted: CAC42883–version 1 and CAC42882–version 2 (Fig. 4 B). These forms differ in their NH_2-terminal regions (upstream of the residues VINK) and by the presence of a 37–amino acid sequence in the COOH-terminal half of version 2 found in all the other eukaryotic orthologues so far (between the residues EDTG:RQML). We generated an antibody to amino acids 327 to 629 of HsIX-14.v1 (downstream of the catalytic motif). As this region is fully present in both predicted human versions, the antibody should recognize the two forms if they indeed both exist. Fig. 8 A shows a typical staining pattern observed with the $HsIX\text{-}14^{327\text{-}629}$ antibody in HeLa cells. We observed unusual ring-like structures similar to those seen with the EGFP-tagged protein. These striking structures were also observed in two other human transformed cell lines, Jurkat and CF-PAC (unpublished data). These structures were observed in all interphase cells, and although their size remained fairly constant (<1 μm in diameter), the number of the structures varied on a cell to cell basis. Z-series of sections through cells showed that these structures were located in the lower third of the cells. Because the ring-like structures were dispersed in mitosis in all cell types examined, we believe that the localization (and/or activity) of IX-14 may be regulated during the cell cycle.

Although proteases are found in diverse structures within cells, this particular localization did not resemble any of the usual protease-containing complexes, e.g., 26S proteasome, the related COP9–signalosome complex, lysosomes, or aggresomes. Nonetheless, we performed colocalization immunofluorescence with antibodies to IX-14 and proteasome core subunits α5 and β5i, signalosome subunit Cgn3, chaperone protein Hsc70, and markers for Golgi, mitochondria, and lysosomes. We observed no significant colocalization between IX-14 and any of these proteins (unpublished data). However, numerous transformed cells contain invadopodia, which are believed to be important for extracellular matrix degradation and cellular migration (Bowden et al., 1999, 2001; Baldassarre et al., 2003; Buccione et al., 2004). Invadopodia resemble in size and distribution the structures labeled by the IX-14 antibody. As no proteins exclusive to invadopodia have yet been identified, definitive colocalization was not possible. However, we detected limited colocalization with markers shown to label invadopodia (e.g., phosphotyrosine, cortactin, and Dynamin 2), suggesting that these cytoplasmic ring-like structures very likely are invadopodia.

A role for IX-14 in cell migration

If IX-14 were involved in cell migration, as suggested by the invadopodia-like localization, one might predict that the protein should localize to regions of cells actively involved in migration. Thus, we examined the localization in stationary and migrating human macrophages (Fig. 8, B and C). Fig. 8 B showed that punctate, at times ring-like, cytoplasmic IX-14 structures were observed in cultured human macrophages (in the example shown, the cell is stationary). The morphology of macrophages is dramatically altered as they migrate. In the two examples shown, the IX-14 protein is strikingly mobilized from internal structures to the leading edge of cells (Fig. 8 C). This extraordinary relocalization of IX-14 protein suggests a very intimate involvement of this protein in cell migration.

Given a possible role for this protein in cell migration, we examined primordial germ cell migration in wild-type and *IX-14* mutant *Drosophila* embryos (for review see Santos and Lehmann, 2004). After being the first cells to form very early in embryogenesis, primordial germ cells are passively carried along the dorsal side of the embryo in close association with the posterior midgut primordium. As this primordium invaginates, the germ cells are carried to the interior of the embryo. After this, they actively migrate away from the midgut toward

Published November 22, 2004

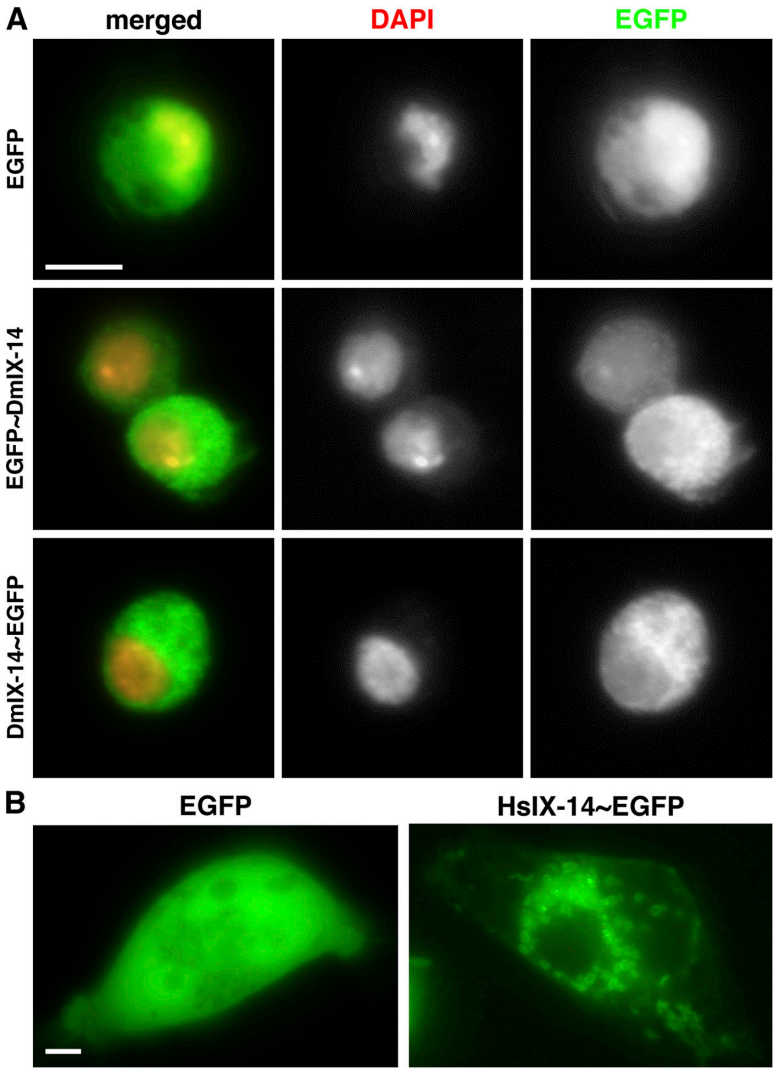

Figure 7. **Localization of GFP-tagged IX-14 in *Drosophila* S2 and HeLa cells.** (A) *Drosophila* S2 cells transiently transfected with constructs expressing EGFP vector only (top) and DmIX-14 tagged at the NH_2 (middle) and COOH termini (bottom). EGFP, green; DAPI, red. DmIX-14 tagged with EGFP at either end appears to be concentrated in cytoplasmic foci, in contrast to EGFP alone, which shows diffuse localization throughout the cytoplasm and nucleus. Bar, 5 μm. (B) HeLa cells transiently transfected with constructs expressing EGFP vector only (left) or HsIX-14 tagged at the COOH terminus (right). EGFP alone is localized diffusely throughout both nucleus and cytoplasm, HsIX-14~EGFP is localized to cytoplasmic ring-like structures. Bar, 5 μm.

the adjacent mesoderm where they associate with somatic gonadal precursor cells. These clusters of cells further migrate and coalesce into gonads later in embryogenesis. Using Vasa as a marker for primordial germ cells, we examined embryos both before and after the migration phases. As shown in Fig. 9, germ cells in both wild-type (Fig. 9 A, top) and mutant (Fig. 9 B, top) embryos are similarly dispersed at the stage before active migration. However, a dramatic difference is seen in embryos at the later stage of gonad coalescence, with gonads visible in wild type (Fig. 9 A, bottom), but not in the mutation (Fig. 9 B, bottom). Mutant larvae then lack gonads (unpublished data). Therefore, the IX-14 protease is playing a role in cell migration, as well as in mitosis, in *Drosophila*.

Discussion

Drosophila IX-14 mutations cause a variety of defects in chromosome, spindle, and nuclear envelope structure during mitosis. Here, we have shown that the *IX-14* gene encodes a novel metalloprotease that is highly conserved in metazoa. Because of its homology to leishmanolysin, we suggest that the core of the IX-14 protease should structurally resemble that of leishmanolysin. In both *Drosophila* and human cells, the metalloprotease is concentrated in cytoplasmic organelles that we believe correspond to invadopodia. In recognition of the homology and intracellular distribution, we have termed the IX-14 enzyme invadolysin.

Three lines of evidence point to invadolysin activity as being crucially involved in the mitotic structural defects observed in *Drosophila IX-14* neuroblasts: (1) The mRNA for the *IX-14* gene is absent from larval tissues of two independently generated mutations, both of which have identical phenotypes; (2) dsRNA-mediated depletion of the IX-14 protein in cultured cells mimics the specific spindle and centrosome defects initially observed in the animal; and (3) in zymography experiments, mutant larval brains lack protease activity that is present in wild-type tissues.

Our analysis of the phenotype of *IX-14* mutant alleles of *Drosophila* revealed that lamin (both Dm0 and C) and otefin proteins are present in elevated amounts in mutant neuroblasts. This finding suggests that invadolysin or one of its downstream targets normally promotes the turnover of these nuclear envelope proteins. In fact, cleavage may be due to invadolysin itself, as we have shown that the enzyme can cleave *Drosophila*

Published November 22, 2004

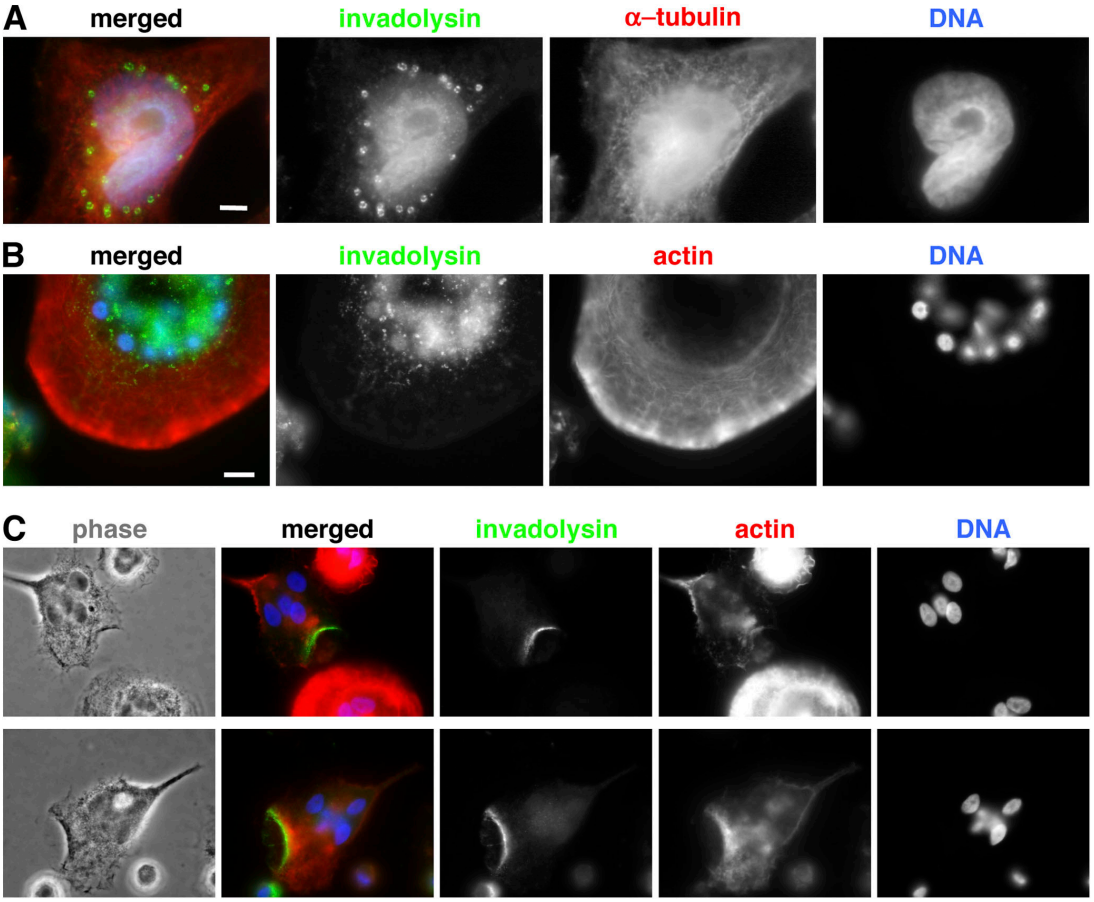

Figure 8. **Localization of IX-14/invadolysin in human cells.** (A) HsIX-14 localization in HeLa cells, detected with a rabbit antibody generated to HsIX-14 (amino acids 327–629). HsIX-14, green; α-tubulin, red; DAPI, blue. The HsIX-14 staining is seen as discrete ring-like structures in the cytoplasm of interphase cells, in addition to a nuclear pool of the protein. This staining pattern becomes more diffuse in mitosis, and is similar in Jurkat and CF-PAC cells (not depicted). Bar, 5 μm. (B) HsIX-14 localization in normal stationary human macrophages cultured in vitro. HsIX-14, green; rhodamine-phalloidin/actin, red; DAPI blue. Bar, 5 μm. (C) HsIX-14 localization in normal migrating human macrophages cultured in vitro. HsIX-14, green; rhodamine-phalloidin/actin, red; DAPI, blue. Note that all of the IX-14/invadolysin has now strikingly relocalized to the leading edge of the cells.

lamin Dm0 in vitro. Many previous papers have demonstrated that lamina dynamics in mitosis are regulated by reversible phosphorylation by Cdk1:cyclin B and that the proteins are reused at nuclear envelope reformation during telophase (Gant and Wilson, 1997). Thus, although the mechanism and timing of the invadolysin-dependent nuclear envelope turnover has yet to be determined, the phenomenon is important because it reveals previously unsuspected complexities of nuclear envelope dynamics during the cell cycle. Identification of other invadolysin substrates, e.g., ones essential for chromosome condensation and spindle assembly, will also illuminate further details of these mitotic rearrangements.

The IX-14 gene encodes a novel metalloprotease

Sequence analysis of the *IX-14* gene suggested that it encodes a novel conserved zinc-metalloprotease with sequence homology to leishmanolysin and to orthologues that we have identified in a range of metazoan species. Leishmanolysin is a major cell surface protease that is required for *Leishmania's* parasitic activity. It has been extensively studied due to its pathogenic role in leishmaniasis (Russell and Wilhelm, 1986; Yang et al., 1990; Connell et al., 1993; Xu and Liew, 1995; McGwire and Chang, 1996; Yao et al., 2003), and has also recently been shown to enhance migration of *Leishmania* through extracellular matrix (McGwire et al., 2003).

Like leishmanolysin, invadolysin has the conserved residues of the metzincin protease "HEXXHXXG[X]$_N$H" motif. This motif has been characterized in detail by mutational analysis of the three conserved histidine (which coordinate the zinc ion) and glutamic acid residues, which are absolutely required for catalytic activity (McMaster et al., 1994; Macdonald et al., 1995; McGwire and Chang, 1996). We additionally noted the conserved spacing of 14 cysteines among leishmanolysin and the orthologues described in this paper. Molecular modeling studies revealed that the framework of the higher eukaryotic form of this protein is likely to closely resemble that of leishmanolysin, with differences being confined to surface features that likely mediate interactions with substrates, regulators, and/or other binding partners.

None of the identified invadolysin orthologues has had any functions ascribed to them. Therefore, we propose that the IX-14/invadolysin family is required for cell cycle structural rearrangements, a novel activity for this class of proteases. The Zmpste24

Published November 22, 2004

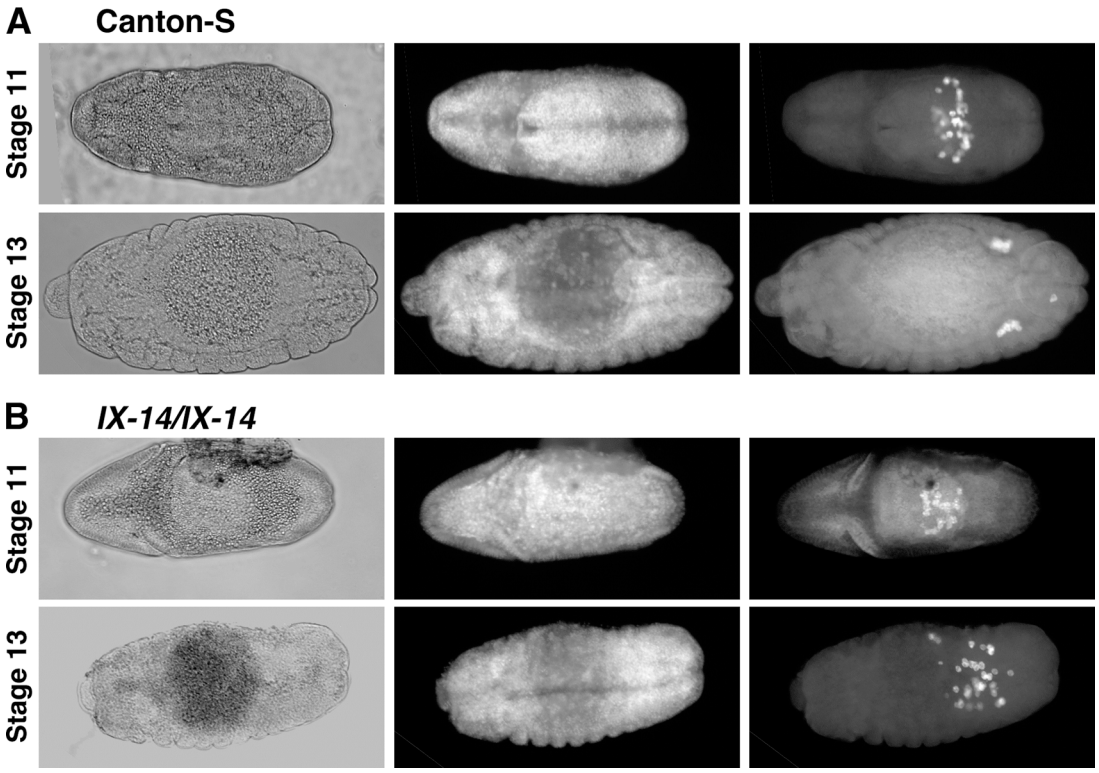

Figure 9. **Germ cell migration defects in *l(3)IX-14* embryos.** All panels are dorsal views of *Drosophila* embryos. Left panels are phase-contrast images, middle panels show DAPI labeling of DNA, right panels show germ cells detected by Vasa antibody. (A) Wild-type Canton S embryos. (top) Stage 10/11, when germ cells are in the middle of passing through the midgut and migrating dorsally. (bottom) Stage 13, when germ cells form two elongated clusters on either side of the embryo. (B) *IX-14* homozygous embryos selected for absence of the Kr-GFP balancer chromosome. (top) Stage 10/11, germ cells appear as in wild-type embryos. (bottom) Stage 13, when the abnormal germ cell migration phenotype is apparent. The germ cells fail to migrate and coalesce into gonads.

metalloprotease in mice (a member of the M48 family of zinc-metalloproteases) has a role in prelamin A cleavage (Pendas et al., 2002). Matrix metalloproteases (MMPs) have been implicated in remodeling of the extracellular matrix (Ishizuya-Oka et al., 2000) and in release of growth factors (Levi et al., 1996). MMPs have been shown to act in some cancers to digest the surrounding extracellular matrix and aid the process of metastasis (Ellerbroek and Stack, 1999; Horikawa et al., 2000; Johansson et al., 2000). Whereas the human genome encodes 24 MMPs, *Drosophila* has only two MMP genes: Dm1-MMP is expressed more specifically during embryonic stages and Dm2-MMP apparently throughout development (Llano et al., 2000, 2002). Few mutations are available to study metalloproteases in a developing organism, although a study on double mutants of the two *Drosophila* MMPs has shown that whereas tissue remodeling is disrupted, embryonic development and larval mitosis are unaffected (Page-McCaw et al., 2003). Thus, no other metalloprotease affects cell proliferation as IX-14/invadolysin does.

Intracellular localization of IX-14 to invadopodia

Although a nuclear pool of invadolysin is detectable in human cells, protein is also localized to the cytoplasm in both fly and human cells, where it is concentrated in unusual ring-like structures. These structures are observed during interphase in all human cultured cells examined, but become dispersed during mitosis, when the protein adopts a more diffuse distribution. We believe the ring-like structures represent invadopodia, cytoplasmic structures that have been proposed to have an important role in cell migration and metastasis. Like invadopodia, the ring-like structures containing invadolysin are localized to the lower third of the cell close to the substratum. They also contain cortactin, paxillin, and dynamin 2, previously shown to be enriched in invadopodia. Intriguingly, dynamin 2, which is also found in invadopodia, has been recently shown to play a role in centrosome cohesion (Thompson et al., 2004), thus tying in with our results linking migration with mitosis.

Strikingly, although invadolysin has a punctate cytoplasmic localization in stationary macrophages, when actively migrating macrophages are visualized, invadolysin becomes strongly concentrated at the leading edge of the cell. How this relocalization occurs will be investigated in living cells, coupled with an analysis of extracellular matrix degradation. Invadolysin appears to be the first specific marker for invadopodia as a discrete cytoplasmic compartment, and, as such, will be a key potential target for drugs designed to limit cell migration.

Analysis of invadolysin mutants identifies a previously unsuspected role for metalloproteases in cell division and development

The *IX-14* mutation in *Drosophila* causes cells to arrest in mitosis with hypercondensed mitotic chromosomes surrounded by poorly condensed chromatin, a phenotype that is clearly dis-

Published November 22, 2004

tinct from the chromosome hypercondensation commonly observed in mutations exhibiting mitotic delay (Heck et al., 1993; Theurkauf and Heck, 1999). Invadolysin also appears to have a role in chromosome architecture during interphase because mutations exhibit poorly structured polytene chromosomes and have compromised heterochromatin, as assayed by position effect variegation. The levels of nuclear lamin and otefin proteins are dramatically increased in mutant mitotic cells. One possibility suggested by these results is that invadolysin might regulate interactions between chromatin and the nuclear envelope that are important for gene expression and/or mitotic chromosome condensation. Invadolysin could have a direct role on components such as topoisomerase II or condensin, or the effects we have observed could result from disruption of a novel pathway in which proteolysis plays a role.

In addition, invadolysin has nonchromosomal roles, as both centrosome duplication and/or separation and mitotic spindle formation are aberrant in mutant neuroblasts. Thus, the phenotypes resulting from loss of invadolysin are novel and distinct from other previously described mitotic defects. We have presented evidence that the protein is involved in migration of human macrophages and fly primordial germ cells. Thus the identification and study of this gene has provocatively linked mitosis with cell migration.

A simplistic hypothesis is that different forms of the protein may be important for structural rearrangements during the cell cycle and for cellular migration. Clearly, the generation of reagents recognizing specific forms would be required to address this question. Differential regulation of the expression or localization of these forms could be used during development and/or disease pathogenesis. It is clear from the striking phenotype displayed by *IX-14* mutations that invadolysin illuminates a previously unsuspected pathway essential for cell division and development in metazoa. Future identification of invadolysin substrates will help to clarify the role of this protein and lead to better understanding of the ways in which structural changes during the cell cycle may be coordinated with cell movements.

Materials and methods

Drosophila stocks

The wild-type strain used was Canton S. We received *l(3)IX-14*^{1} from M. Gatti (University of Rome, Rome, Italy); it was originally generated in an ICR-170 screen by A. Shearn (Johns Hopkins University, Baltimore, MD). We generated *l(3)IX-14*^{4Y7} after local hopping a nearly P transposon insertion, *l(3)04017*, obtained from the Bloomington Stock Center.

DAPI staining of *Drosophila* neuroblast squashes and polytene chromosomes

Brains or salivary glands from third instar larvae were processed as described previously (Heck et al., 1993; Loupart et al., 2000) and mounted in Mowiol/glycerol. Fluorescence was observed using a fluorescence microscope (model AX-70 Provis; Olympus) fitted with epifluorescence filters (Chroma Technology Corp.). Digital images were captured (at ~18°C) using a camera (model Orca II; Hamamatsu) with Vysis QUIPS software and processed using Adobe Photoshop 4.0.

Immunofluorescence of third instar larval brains

Analysis of α-tubulin (Sigma-Aldrich), CP190 (provided by W. Whitfield, University of Dundee, Dundee, Scotland), lamin (provided by P. Fisher, State University of New York at Stony Brook, Stony Brook, NY), otefin (provided by Y. Gruenbaum, Hebrew University of Jerusalem, Jerusalem, Israel), cyclin B (provided by J. Raff, University of Cambridge, Cambridge, England), and P~H3 (Upstate Biotechnology) antibodies in third instar larval brains was performed as described previously (Bonaccorsi et al., 2000). BrdU incorporation and subsequent detection by a rat anti-BrdU antibody (Harlan Sera) in larval brains was performed as described previously (Loupart et al., 2000). Imaging was performed as detailed in the previous section.

Immunoblotting

Protein extracts were electrophoresed on Novex SDS-PAGE gels (Invitrogen), and then transferred to nitrocellulose membrane (Schleicher and Schuell). Membranes were rinsed for 5 min with PBS-Tw (PBS + 0.1% Tween 20), and then blocked for 1 h with Safeway dried skimmed milk (5% in PBS-Tw) at RT with shaking. Primary and secondary antibody incubations were performed in PBS-Tw for 1 h at RT with shaking, with washes of 2 × 3 min, 1 × 15 min, and then 2 × 5 min after each incubation. Chemiluminescent detection of HRP-conjugated secondary antibody was performed using ECL reagents from Amersham Biosciences, according to the manufacturer's instructions.

Northern blotting

Northern blots were performed as described in Sambrook et al. (1989). Total RNA was prepared from homogenized third instar larvae using the RNeasy RNA extraction kit (QIAGEN). 10 μg of total RNA per lane was electrophoresed on a 1% agarose gel. RNA was transferred to nylon membrane by capillary action with 20× SSC overnight. RNA was subsequently UV-cross-linked to the membrane using a Strata-linker (Stratagene). Hybridization of ^{32}P-dCTP (AP Biotech)–labeled probes at a specific activity of at least 10^6 counts per milliliter was performed at 65°C overnight as described in Church and Gilbert (1984). The HighPrime kit (Boehringer) was used for all random primer labeling. Autoradiography was done at −80°C using XAR-5 film (Kodak).

dsRNA-mediated interference

dsRNAi was performed on *Drosophila* S2 cells as described previously (Clemens et al., 2000; Vass et al., 2003), using 15 μg/ml of double stranded IX-14 RNA per 2 ml of cells at 10^6 cells/ml.

Immunofluorescence of *Drosophila* S2 and HeLa cultured cells

S2 cells were grown on either Permanox Chamber Slides (Lab-Tek) for the RNAi experiments or on poly-L-lysine coverslips in 6-well plates for the EGFP-fusion detection using a rabbit anti-GFP antibody (Molecular Probes). HeLa cells were grown on coverslips in 6-well plates for transfection with EGFP fusion constructs. For immunofluorescence, cells were fixed with 4% PFA in PBS for 3 min, permeabilized in PBS + 0.5% Triton X-100 for 1 min, and washed 2 × 10 min incubations in PBTx. The cells were blocked for 1 h in 3% BSA in PBS at RT. Primary antibody incubation was overnight at 4°C in 0.3% BSA in PBS. Cells were washed 3 × 5 min in PBTx, followed by secondary antibody incubation for 1 h at 37°C (secondary antibodies incubated separately). Final washes were 3 × 5 min in PBTx, with the penultimate wash containing 0.1 μg/ml DAPI, and the coverslips were mounted in Mowiol-glycerol. Imaging was performed as detailed in the section DAPI staining of *Drosophila* neuroblast squashes and polytene chromosomes.

Detection of protease activity by zymography

Zymogram gels (Novex) containing casein as a substrate were used for all zymography. Wandering third instar larvae were dissected in 1× EBR. Brains were transferred to 50 μl of chilled EBR, and then homogenized for ~30–60 s with a hand-held homogenizer. 50 μl of 2× Tris-glycine gel sample buffer (Novex) plus 1 mM DTT was added, and the samples were incubated for 10 min at RT. Samples (without boiling) were loaded onto 12% Tris-Glycine Zymogram gels and electrophoresed at 125 V constant, generally for 3–4 h, at least until the dye front had run off the gel. After electrophoresis, gels were rinsed in renaturing buffer (2.5% Triton X-100) for 30 min, equilibrated in Developing buffer (Novex) for 30 min, and incubated overnight at 37°C in Developing buffer. Gels were stained with Colloidal Coomassie blue (Sigma-Aldrich) to visualize the casein in the gel.

in vitro proteolysis of lamin by invadolysin

375 ng of Lamin in T7-7 vector, IX-14 in pOT2 vector, or GFP control vector was added to one 24-μl aliquot of the RTS 500 *Escherichia coli* Circular Template kit (Roche). Each expression aliquot was incubated in a water bath at 30°C for 1 h. 10 μl of IX-14 was mixed with 1 or 4 μl of lamin or GFP before being incubated in a water bath at either 29 or 37°C for

Published November 22, 2004

15 min, 50 min, or 1 h. In some cases, the incubation was with $ZnCl_2$ or $ZnSO_4$ or the zinc chelator 1,10-phenanthroline. After the reaction, samples were boiled at 100°C for 5 min in SDS-PAGE sample buffer. Lamin was detected after blotting to nitrocellulose using an mAb generated to the *Drosophila* NH_2-terminal head region (amino acids 22–28).

Macrophage isolation and culture

Macrophages were isolated from normal human blood following the procedure of Giles et al. (2001). After isolation, the mononuclear cells were plated at 4×10^6/ml in Iscoves' modified Dulbecco's medium (with L-glut and 25 mM Hepes) onto glass coverslips in 12-well tissue culture plastic plates for 1 h. Adherence to the glass coverslips was used to enrich for the monocytes out of the lymphocytes/monocytes mix (lymphocytes do not attach). After settling, the plates were washed in Hank's Balanced Salt Solution (without divalent cations) to remove nonadherent lymphocytes, and then 2 ml of Iscoves' modified Dulbecco's medium + 10% autologous serum was added and the cells were cultured at 37°C, 5% CO_2, for 5 d. After 5 d, the cells were washed again to remove any nonadherent cells and fixed in 3% PFA at RT for 20 min. After washes in PBS, 50 mM NH_4Cl was added to the wells for 15 min. Coverslips were permeabilized in 0.1% Triton X-100 for 4 min. After washes, the cells were blocked in 10% heat-inactivated human serum and processed for immunofluorescence as usual.

Detection of germ cells

For the examination of appropriately staged embryos, Canton S wild-type and 4Y7/TM3 (Kr:GFP) flies were allowed to lay embryos on yeasted red wine concentrate agar plates either overnight or for 3-h collections, which were then aged until the desired stage. Embryos were washed and dechorionated in 50% bleach in ddH_2O for 4 min and rinsed. Homozygous 4Y7/4Y7 embryos were hand selected (fluorescence microscopy) by virtue of lacking the Kr-GFP expression pattern (visible after stage 9; Casso et al., 2000). The selected embryos were fixed in PFA, permeabilized by heptane, devitellinized by methanol, and rehydrated as described previously (Theurkauf and Heck, 1999). After a block in 1% BSA in PBS for 1 h, rabbit Vasa antibody (provided by P. Lasko, McGill University, Montreal, Canada) was used as 1:500 in PBS + 0.3% Triton X-100 overnight at 4°C. Alexa-594–conjugated secondary antibody was used as 1:500 in PBSTx for 2 h at RT. 4×15 min PBSTx washes were performed before and after antibody incubations. DAPI at 0.1 μg/ml DAPI was included in the penultimate wash. Embryos were mounted with Vectashield and imaged as detailed in the section DAPI staining of *Drosophila* neuroblast squashes and polytene chromosomes.

Online supplemental material

Further details on TUNEL labeling of larval brains, dsRNA-mediated interference in S2 cells, and cultured cell transfections (*Drosophila* and HeLa) are provided online. Online supplemental material is available at http://www.jcb.org/cgi/content/full/jcb.200405155/DC1.

We would like to thank Allen Shearn and Maurizio Gatti for enthusiastically encouraging our progress in this project. Marie-Louise Loupart, Alison Wilkie, Liping Lu, Lynne Cursiter, Sophie Lecomte, and Tina Volaki are all to be acknowledged for technical and intellectual contributions during honors and other projects. We are grateful to the following individuals for generous gifts of antibody: Paul Fisher, Yoshef Gruenbaum, Paul Lasko, Mark McNiven (Dynamin, Mayo Clinic, Rochester, NY), Jordan Raff, and Will Whitfield. Victor Simossis was instrumental in generating the T-COFFEE alignment. M. Heck thanks Susette Mueller (Georgetown University, Washington, DC) for suggesting the examination of macrophages and Ian Dransfield (University of Edinburgh, Edinburgh, UK) for the culturing of macrophages.

Brian McHugh was supported by a Prize Studentship and a Prize Fellowship from the Wellcome Trust. Research in the Heck laboratory is supported by a Senior Research Fellowship in the Biomedical Sciences from the Wellcome Trust.

Submitted: 26 May 2004
Accepted: 4 October 2004

References

Baldassarre, M., A. Pompeo, G. Beznoussenko, C. Castaldi, S. Cortellino, M.A. McNiven, A. Luini, and R. Buccione. 2003. Dynamin participates in focal extracellular matrix degradation by invasive cells. *Mol. Biol. Cell.* 14:1074–1084.

Bhat, M.A., A.V. Philp, D.M. Glover, and H.J. Bellen. 1996. Chromatid segregation at anaphase requires the barren product, a novel chromosome-associated protein that interacts with topoisomerase II. *Cell.* 87:1103–1114.

Bonaccorsi, S., M.G. Giansanti, and M. Gatti. 2000. Spindle assembly in *Drosophila* neuroblasts and ganglion mother cells. *Nat. Cell Biol.* 2:54–56.

Bowden, E.T., M. Barth, D. Thomas, R.I. Glazer, and S.C. Mueller. 1999. An invasion-related complex of cortactin, paxillin and PKCmu associates with invadopodia at sites of extracellular matrix degradation. *Oncogene.* 18:4440–4449.

Bowden, E.T., P.J. Coopman, and S.C. Mueller. 2001. Invadopodia: unique methods for measurement of extracellular matrix degradation in vitro. *Methods Cell Biol.* 63:613–627.

Buccione, R., J.D. Orth, and M.A. McNiven. 2004. Foot and mouth: podosomes, invadopodia, and circular dorsal ruffles. *Nat. Rev. Mol. Cell Biol.* 5:647–657.

Casso, D., F. Ramirez-Weber, and T.B. Kornberg. 2000. GFP-tagged balancer chromosomes for *Drosophila melanogaster. Mech. Dev.* 91:451–454.

Church, G.M., and W. Gilbert. 1984. Genomic sequencing. *Proc. Natl. Acad. Sci. USA.* 81:1991–1995.

Clemens, J.C., C.A. Worby, N. Simonson-Leff, M. Muda, T. Maehama, B.A. Hemmings, and J.E. Dixon. 2000. Use of double-stranded RNA interference in *Drosophila* cell lines to dissect signal transduction pathways. *Proc. Natl. Acad. Sci. USA.* 97:6499–6503.

Coelho, P.A., J. Queiroz-Machado, and C.E. Sunkel. 2003. Condensin-dependent localisation of topoisomerase II to an axial chromosomal structure is required for sister chromatid resolution during mitosis. *J. Cell Sci.* 116:4763–4776.

Connell, N.D., E. Medina-Acosta, W.R. McMaster, B.R. Bloom, and D.G. Russell. 1993. Effective immunization against cutaneous leishmaniasis with recombinant bacille Calmette-Guerin expressing the *Leishmania* surface proteinase gp63. *Proc. Natl. Acad. Sci. USA.* 90:11473–11477.

Edgar, B.A., and C.F. Lehner. 1996. Developmental control of cell cycle regulators: a fly's perspective. *Science.* 274:1646–1652.

Ellerbroek, S.M., and M.S. Stack. 1999. Membrane associated matrix metalloproteinases in metastasis. *Bioessays.* 21:940–949.

Fogarty, P., S.D. Campbell, R. Abu-Shumays, B.S. Phalle, K.R. Yu, G.L. Uy, M.L. Goldberg, and W. Sullivan. 1997. The *Drosophila* grapes gene is related to checkpoint gene chk1/rad27 and is required for late syncytial division fidelity. *Curr. Biol.* 7:418–426.

Gant, T.M., and K.L. Wilson. 1997. Nuclear assembly. *Annu. Rev. Cell Dev. Biol.* 13:669–695.

Gatti, M., and B.S. Baker. 1989. Genes controlling essential cell-cycle functions in *Drosophila melanogaster. Genes Dev.* 3:438–453.

Giles, K.M., K. Ross, A.G. Rossi, N.A. Hotchin, C. Haslett, and I. Dransfield. 2001. Glucocorticoid augmentation of macrophage capacity for phagocytosis of apoptotic cells is associated with reduced p130Cas expression, loss of paxillin/pyk2 phosphorylation, and high levels of active Rac. *J. Immunol.* 167:976–986.

Glover, D.M., M.H. Leibowitz, D.A. McLean, and H. Parry. 1995. Mutations in aurora prevent centrosome separation leading to the formation of monopolar spindles. *Cell.* 81:95–105.

Heck, M.M.S., A. Pereira, P. Pesavento, Y. Yannoni, A.C. Spradling, and L.S.B. Goldstein. 1993. The kinesin-like protein KLP61F is essential for mitosis in *Drosophila. J. Cell Biol.* 123:665–679.

Horikawa, T., T. Yoshizaki, T.S. Sheen, S.Y. Lee, and M. Furukawa. 2000. Association of latent membrane protein 1 and matrix metalloproteinase 9 with metastasis in nasopharyngeal carcinoma. *Cancer.* 89:715–723.

Hudson, D.F., P. Vagnarelli, R. Gassmann, and W.C. Earnshaw. 2003. Condensin is required for nonhistone protein assembly and structural integrity of vertebrate mitotic chromosomes. *Dev. Cell.* 5:323–336.

Ishizuya-Oka, A., Q. Li, T. Amano, S. Damjanovski, S. Ueda, and Y.B. Shi. 2000. Requirement for matrix metalloproteinase stromelysin-3 in cell migration and apoptosis during tissue remodeling in *Xenopus laevis. J. Cell Biol.* 150:1177–1188.

Jager, H., A. Herzig, C.F. Lehner, and S. Heidmann. 2001. *Drosophila* separase is required for sister chromatid separation and binds to PIM and THR. *Genes Dev.* 15:2572–2584.

Johansson, N., M. Ahonen, and V.M. Kahari. 2000. Matrix metalloproteinases in tumor invasion. *Cell. Mol. Life Sci.* 57:5–15.

Krause, S.A., M.-L. Loupart, S. Vass, S. Schoenfelder, S. Harrison, and M.M.S. Heck. 2001. Loss of cell cycle checkpoint control in *Drosophila* Rfc4 mutants. *Mol. Cell. Biol.* 21:5156–5168.

Levi, E., R. Fridman, H. Miao, Y. Ma, A. Yayon, and I. Vlodavsky. 1996. Matrix metalloproteinase 2 releases active soluble ectodomain of fibroblast growth factor receptor 1. *Proc. Natl. Acad. Sci. USA.* 93:7069–7074.

Llamazares, S., A. Moreira, A. Tavares, C. Girdham, B.A. Spruce, C. Gonzalez, R.E. Karess, D.M. Glover, and C.E. Sunkel. 1991. Polo encodes a pro-

tein kinase homolog required for mitosis in *Drosophila*. *Genes Dev.* 5:2153–2165.

Llano, E., A.M. Pendas, P. Aza-Blanc, T.B. Kornberg, and C. Lopez-Otin. 2000. Dm1-MMP, a matrix metalloproteinase from *Drosophila* with a potential role in extracellular matrix remodeling during neural development. *J. Biol. Chem.* 275:35978–35985.

Llano, E., G. Adam, A.M. Pendas, V. Quesada, L.M. Sanchez, I. Santamaria, S. Noselli, and C. Lopez-Otin. 2002. Structural and enzymatic characterization of *Drosophila* Dm2-MMP, a membrane-bound matrix metalloproteinase with tissue-specific expression. *J. Biol. Chem.* 277:23321–23329.

Loupart, M.-L., S.A. Krause, and M.M.S. Heck. 2000. Aberrant replication timing induces defective chromosome condensation in *Drosophila* ORC2 mutants. *Curr. Biol.* 10:1547–1556.

Macdonald, M.H., C.J. Morrison, and W.R. McMaster. 1995. Analysis of the active site and activation mechanism of the *Leishmania* surface metalloproteinase GP63. *Biochim. Biophys. Acta.* 1253:199–207.

McGwire, B.S., and K.P. Chang. 1996. Posttranslational regulation of a *Leishmania* HEXXH metalloprotease (gp63). The effects of site-specific mutagenesis of catalytic, zinc binding, N-glycosylation, and glycosyl phosphatidylinositol addition sites on N-terminal end cleavage, intracellular stability, and extracellular exit. *J. Biol. Chem.* 271:7903–7909.

McGwire, B.S., K.P. Chang, and D.M. Engman. 2003. Migration through the extracellular matrix by the parasitic protozoan *Leishmania* is enhanced by surface metalloprotease gp63. *Infect. Immun.* 71:1008–1010.

McMaster, W.R., C.J. Morrison, M.H. MacDonald, and P.B. Joshi. 1994. Mutational and functional analysis of the *Leishmania* surface metalloproteinase GP63: similarities to matrix metalloproteinases. *Parasitology.* 108: S29–S36.

Murray, A.W. 2004. Recycling the cell cycle: cyclins revisited. *Cell.* 116:221–234.

O'Farrell, P.H., B.A. Edgar, D. Lakich, and C.F. Lehner. 1989. Directing cell division during development. *Science.* 246:635–640.

Page-McCaw, A., J. Serano, J.M. Sante, and G.M. Rubin. 2003. *Drosophila* matrix metalloproteinases are required for tissue remodeling, but not embryonic development. *Dev. Cell.* 4:95–106.

Pendas, A.M., Z. Zhou, J. Cadinanos, J.M. Freije, J. Wang, K. Hultenby, A. Astudillo, A. Wernerson, F. Rodriguez, K. Tryggvason, and C. Lopez-Otin. 2002. Defective prelamin A processing and muscular and adipocyte alterations in Zmpste24 metalloproteinase-deficient mice. *Nat. Genet.* 31:94–99.

Pflumm, M.F., and M.R. Botchan. 2001. Orc mutants arrest in metaphase with abnormally condensed chromosomes. *Development.* 128:1697–1707.

Russell, D.G., and H. Wilhelm. 1986. The involvement of the major surface glycoprotein (gp63) of *Leishmania* promastigotes in attachment to macrophages. *J. Immunol.* 136:2613–2620.

Sambrook, J., E.F. Fritsch, and T. Maniatis. 1989. Molecular Cloning: A Laboratory Manual. Cold Spring Harbor Laboratory Press, Cold Spring Harbor, NY. 7.39–7.52.

Santos, A.C., and R. Lehmann. 2004. Germ cell specification and migration in *Drosophila* and beyond. *Curr. Biol.* 14:R578–R589.

Schlagenhauf, E., R. Etges, and P. Metcalf. 1998. The crystal structure of the *Leishmania major* surface proteinase leishmanolysin (gp63). *Structure.* 6:1035–1046.

Shearn, A., T. Rice, A. Garen, and W. Gehring. 1971. Imaginal disc abnormalities in lethal mutants of *Drosophila. Proc. Natl. Acad. Sci. USA.* 68: 2594–2598.

Sibon, O.C.M., V.A. Stevenson, and W.E. Theurkauf. 1997. DNA-replication checkpoint control at the *Drosophila* midblastula transition. *Nature.* 388: 93–97.

Steffensen, S., P.A. Coelho, N. Cobbe, S. Vass, M. Costa, B. Hassan, S.N. Prokopenko, H. Bellen, M.M.S. Heck, and C.E. Sunkel. 2001. A role for *Drosophila* SMC4 in the resolution of sister chromatids in mitosis. *Curr. Biol.* 11:295–307.

Sunkel, C., and D.M. Glover. 1988. polo, a mitotic mutant of *Drosophila* displaying abnormal spindle poles. *J. Cell Sci.* 89:25–38.

Theurkauf, W.E., and M.M.S. Heck. 1999. Identification and characterization of mitotic mutations in *Drosophila*. *In* Methods in Cell Biology. Vol. 61. C.L. Rieder, editor. Academic Press, Inc., San Diego, CA. 317–346.

Thompson, H.M., H. Cao, J. Chen, U. Euteneuer, and M.A. McNiven. 2004. Dynamin 2 binds gamma-tubulin and participates in centrosome cohesion. *Nat. Cell Biol.* 6:335–342.

Vass, S., S. Cotterill, A.M. Valdeolmillos, J.L. Barbero, E. Lin, W.D. Warren, and M.M. Heck. 2003. Depletion of rad21/Scc1 in *Drosophila* cells leads to instability of the cohesin complex and disruption of mitotic progression. *Curr. Biol.* 13:208–218.

Whitfield, W.G.F., M.A. Chaplain, K. Oegema, H. Parry, and D.M. Glover. 1995. The 190 kDa centrosome-associated protein of *Drosophila melanogaster* contains four zinc finger motifs and binds to specific sites on polytene chromosomes. *J. Cell Sci.* 108:3377–3387.

Xu, D., and F.Y. Liew. 1995. Protection against leishmaniasis by injection of DNA encoding a major surface glycoprotein, gp63, of *L. major*. *Immunology.* 84:173–176.

Yang, D.M., N. Fairweather, L.L. Button, W.R. McMaster, L.P. Kahl, and F.Y. Liew. 1990. Oral *Salmonella typhimurium* (AroA-) vaccine expressing a major leishmanial surface protein (gp63) preferentially induces T helper 1 cells and protective immunity against leishmaniasis. *J. Immunol.* 145: 2281–2285.

Yao, C., J.E. Donelson, and M.E. Wilson. 2003. The major surface protease (MSP or GP63) of *Leishmania* sp. Biosynthesis, regulation of expression, and function. *Mol. Biochem. Parasitol.* 132:1–16.